Estimates of Lightning NO_x Production Per Flash from OMI NO_2 and Lightning Observations

Kenneth E. Pickering[1,*], Eric Bucsela[2], Dale Allen[3], Kristin Cummings[3],
Yunyao Li[3], Donald MacGorman[4], Eric Bruning[5]

1. NASA Goddard Space Flight Center, Greenbelt, MD USA
2. SRI, International, Menlo Park, CA USA
3. University of Maryland, College Park, MD USA
4. NOAA National Severe Storms Laboratory, Norman, OK USA
5. Texas Tech University, Lubbock, TX USA

ABSTRACT: A specialized retrieval algorithm for estimates of tropospheric column NO_x due to lightning was developed for the Deep Convective Clouds and Chemistry (DC3) field program, conducted during May and June 2012, using NO_2 retrievals from the Ozone Monitoring Instrument (OMI) on NASA's Aura satellite, which provides once-per-day data from an overpass at ~1:30 PM LST. Two forms of the algorithm have been developed. The first is for active or recently active storms and the second is for relatively clear sky situations. Estimates of stratospheric and tropospheric background NO_2 columns are subtracted from the OMI total column observations and an air mass factor representative of a convective outflow regime was used to convert the residual to vertical columns of lightning NO_x (LNO_x). Four case study storms observed in DC3 were selected to estimate LNO_x production per flash based on a combination of the number of moles of LNO_x indicated by OMI and the contributing flashes recorded by the National Lightning Detection Network (NLDN) and Lightning Mapping Arrays (LMAs). Two cases involved OMI observations over active or very recently active lightning-producing storms. Another two cases involved LNO_x observed in relatively clear skies downwind of storms in the DC3 intensive study regions.

INTRODUCTION

NO_2 and NO (together referred to as NO_x) are trace gases important in ozone chemistry in both the troposphere and stratosphere. Worldwide, anthropogenic emissions of NO_x dominate the NO_x budget. However, considerable uncertainty surrounds emission rates from natural sources (lightning and soil). Lightning is the largest non-anthropogenic source of NO_x in the free troposphere (hereafter, we refer to lightning-generated NO_x as LNO_x). Most estimates of global LNO_x production range from 2 to 8 Tg (N) yr^{-1} [Schumann and Huntrieser, 2007] or about 10–15% of the total NO_x budget. The effects of lightning are felt most strongly in the middle and upper part

* Contact information: Kenneth E. Pickering, NASA Goddard Space Flight Center, Code 614, Greenbelt, MD, USA, Email: Kenneth.E.Pickering@nasa.gov

of the troposphere, where this source plays the dominant role in controlling NO_x and ozone amounts especially in the tropics and at midlatitudes in the summer, despite the greater overall magnitude of the anthropogenic NO_x emissions [R. Zhang et al., 2003]. In this region, NO_x has a lifetime several times longer than the approximate 1-day lifetime in the lower troposphere so that a given amount of LNO_x in the upper troposphere can have a greater impact on ozone chemistry. Ozone is the third most important greenhouse gas [IPCC, 2007], and ozone enhancements near the tropopause have the greatest effect on its radiative forcing. Therefore, additional ozone produced downwind of thunderstorm events is particularly effective in climate forcing.

Two types of information are needed for estimating the global LNO_x source strength: the global flash rate and the production per flash. The global number of flashes is fairly well established as a result of climatologies constructed from satellite sensors such as the Optical Transient Detector (OTD, 1995-2000) [Christian et al., 2003; Boccippio et al., 2000] and the Lightning Imaging Sensor (LIS, 1997 to present) [Christian et al., 2003; Boccippio et al., 2002; Mach et al., 2007]. Therefore, the factor of 4 uncertainty in the range of global LNO_x source strength stems primarily from uncertainty in the NO_x production per flash. There have been several methods used to estimate this quantity: theoretical estimates, laboratory experiments, analysis of aircraft observations, cloud-resolving model simulations constrained by lightning flash observations and anvil NO_x measurements, and analysis of satellite observations (see Table 1). Our group has employed the latter three of these methods in previous analyses of LNO_x production. Under NASA-sponsored work, we have developed a preliminary algorithm for computing LNO_x from OMI observations and have applied it for sets of tropical (Bucsela et al., 2010) and midlatitude convective storms. From Table 1 it can be noted that in general, estimates of average LNO_x production per flash determined for midlatitude and subtropical thunderstorms tend to be larger than for tropical thunderstorms. Huntrieser et al. (2008) have hypothesized that LNO_x production per flash at midlatitudes may be larger than in the tropics due to greater vertical wind shear at higher latitudes, leading to greater flash lengths.

METHODS

Algorithm

The Ozone Monitoring Instrument (OMI) is on NASA's Aura satellite, which is part of NASA's A-Train. It is in a sun-synchronous polar orbit, crossing equator at 1:30pm (LT). NO_2 and other species are retrieved using UV/VIS radiance observations. OMI provided daily global coverage beginning in late 2004. However, a substantial number of the pixels in the field of view became blocked after 2008, reducing the coverage per day. The OMI pixel at nadir is 13 x 24 km; pixels become larger toward the edges of the orbital swath. The NASA standard product retrieval for NO_2 (Bucsela et al., 2013) provides the total slant column amount of NO2 between the satellite and the earth's surface, as well as stratospheric and tropospheric vertical column amounts.

We have developed a special algorithm to retrieve the component of NO_2 due to lightning and convert this to a vertical column of NO_x, as illustrated in the following equation:

Table 1. Some Literature Estimates of LNO_x Production Per Flash

Method	Moles NO/flash (Notes)	Reference
Theoretical	1100 (CG), 110 (IC)	Price et al., 1997
Laboratory	~103	Wang et al., 1998
Aircraft data, cloud model	345-460 (STERAO-A)	DeCaria, et al., 2005
Aircraft data, cloud model	360 (STERAO-A, EULINOX)	Ott et al., 2007; 2010
Aircraft data, cloud model	590-700 (CRYSTAL-FACE)	Ott et al., 2010
	500 (Mean midlat. from model)	Ott et al., 2010
Aircraft data, cloud model	500 - 600 (Hector)	Cummings et al., 2013
Aircraft data	70-210 (TROCCINOX)	Huntrieser et al., 2008
Aircraft data	121-385 (SCOUT-O3 Darwin)	Huntrieser et al., 2009
Aircraft data	70-179 (AMMA)	Huntrieser et al., 2011
LMA/Theoretical	484 (CG), 34 (IC)	Koshak et al., 2013
Satellite (GOME)	32-240 (Sub-Tropical)	Beirle et al., 2006
Satellite (OMI)	87-246 (TC4 – tropical marine)	Bucsela et al., 2010
	174 (TC4 mean from OMI)	Bucsela et al., 2010
Satellite (OMI)	440 (Central US, Gulf)	Pickering et al. (in prep)
Satellite (SCIAMACHY)	33-50 max. (global analysis)	Beirle et al., 2010

$$\Omega_{LNOx} = \frac{\Omega^{slant}_{total} - \Omega^{OMI}_{strat} \times AMF_{strat} - \Omega^{OMI}_{BG} \times AMF_{trop}}{AMF_{LNOx}}$$

In this equation Ω is the column amount (which can be either NO_X or NO_2). The stratospheric column (red) is based on mean OMI stratospheric NO_2 from the standard algorithm for 4 days surrounding day of analysis. The tropospheric background (BG) column (green) is an estimate of the contributions of sources other than lightning to tropospheric column. We use the fraction of the monthly mean tropospheric NO_2 column from the standard algorithm that is not due to lightning as an approximation of the background. For both stratosphere and tropospheric background we use the air mass factors (AMF) supplied by the standard algorithm to convert the vertical columns to slant columns. AMFs result from radiative transfer modeling using an assumed NO_2 profile, cloud information, and surface albedo. The tropospheric background is assumed to be zero for OMI pixels for which the cloud radiative fraction (CRF) is greater than 0.7 (ie., an assumption that the instrument is viewing very little of the pollution in the lower troposphere when substantial highly reflective cloud is present). Following subtraction of the stratospheric and tropospheric background components in the numerator, we divide by an AMF for LNO_X, which assumes a profile shape appropriate for LNO_x (maximum in the upper troposphere). This AMF converts the slant column LNO_2 to vertical column LNO_x. The LNO_x profile shape comes from gridded output from NASA's Global Modeling Initiative (GMI) chemical transport model which was run with and without lightning. Profiles of LNO and LNO_x are obtained by subtracting the profiles from the no-lightning simulation from those from the simulation with lightning. Our algorithm results in vertical LNO_x columns for each OMI pixel. The LNO_x columns are converted to moles of LNO_x and summed over 1 deg x 1 deg grid cells.

Analysis of LNO_x in relation to observed lightning

Four storm cases from the Deep Convective Clouds and Chemistry (DC3) experiment during May-June 2012 were selected for analysis of the OMI LNO_x in relation to observed lightning flashes. These were cases in which DC3 research aircraft conducted flights measuring NO_x in the region with enhanced OMI LNO_x. The in-situ data collected by the aircraft were used in determining the manner in which the tropospheric background and CRF criteria were handled. The OMI data were observed downwind of two storms in relatively clear sky conditions (30 May – downwind of the Oklahoma storm of 29-30 May; 8 June – downwind of Colorado storms of 7-8 June), and in a second two cases the OMI overpass was over active convection (11 June over Missouri, Illinois, and Arkansas and 21 June over Missouri and Illinois). For the downwind cases OMI pixels with CRF < 0.3 were used, and for the active convection cases pixels with CRF > 0.7 were used.

For all four cases back trajectories were constructed from the region of OMI LNO_x enhancement to determine the regions containing lightning flashes that contributed to the enhancement. Flashes are counted along the trajectories. Flashes from the Oklahoma Lightning Mapping Array (LMA) were used for the 29-30 May storm. The 7-8 June storms occurred over the Colorado LMA, but flash data were not yet available for this case. Therefore, in this case, as well as the June 11 and 21 cases over Missouri/Illinois/Arkansas where no LMA exists, cloud-to-ground flash data from the National Lightning Detection Network (NLDN) were used. In these cases total flashes were estimated using the appropriate gridded values of the climatological IC/CG ratio developed by Boccippio et al. (2000). The trajectories were also used to estimate the transport time from the locations where the lightning occurred to the location where the LNO_x was observed by OMI. An exponential decay of LNO_x over the duration of transport was assumed with an upper tropospheric NO_x lifetime of 4 days.

RESULTS

Downwind Cases

Figure 1 shows a radar reflectivity depiction of the Oklahoma storms that occurred on 29-30 May 2012, and the resulting downwind LNO_2 detected on 30 May over the southern Appalachians. In the figures shown here, the LNO_2 has not yet been converted to LNO_x. Figure 2 shows a sample of the estimated total flashes during the 0100 – 0400 UT period of this storm, as well as a sample of the trajectories that link the LNO_2 maximum with these flashes. The LMA network recorded 31,553 flashes over the duration of the storm system that was sampled by the DC3 aircraft (compared with 45,751 flashes when estimating total flashes using the NLDN data scaled using the Boccippio IC/CG ratios). However, the trajectories indicate that other storms in Oklahoma as well as storms in Alabama contributed to the LNO_x maximum over the southern Appalachians. Scaling the total flashes counted along the trajectories using the ratio of LMA to adjusted NLDN flashes for the major Oklahoma storm yields a total of 104, 513 contributing flashes. The LNO_x retrieval produced ~2.9 x 10^7 moles, yielding ~280 moles LNO_x per flash on average.

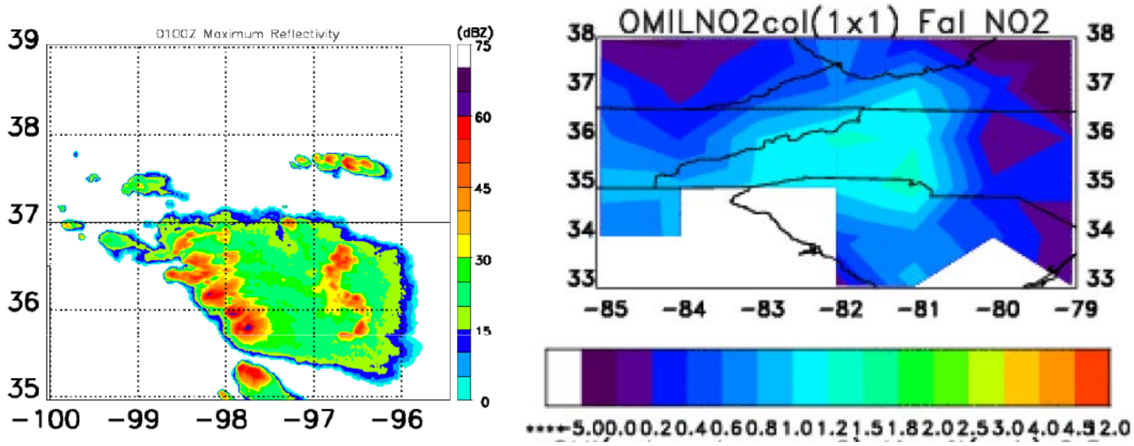

Figure 1. (left) Composite radar reflectivity for major convective system in Oklahoma at 0100 UT on 30 May 2012; (right) OMI LNO_2 maximum over the southern Appalachians at ~1830 UT on 30 May 2012. Units: 10^{15} molecules cm^{-2}.

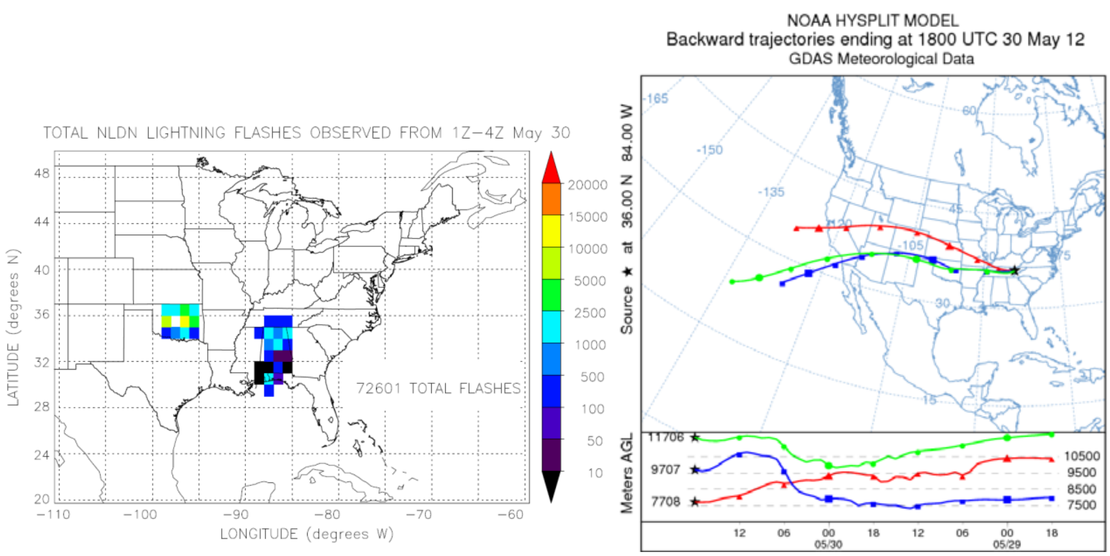

Figure 2. (left) Gridded total flash counts derived from NLDN cloud-to-ground flashes scaled using climatological IC/CG ratios for the period 0100 – 0400 UT on 30 May 2012; (right) back trajectories from region of LNO_x enhancement on 30 May 2012, indicating transport from Oklahoma storm in the 10 – 12 km layer.

A second downwind case (8 June 2012) is in the process of being analyzed. Figure 3 shows the flash distribution for a complex of storm systems over northeastern Colorado, southeastern Wyoming and western Nebraska during the hour between 0100 and 0200 UT and the OMI LNO_2 field showing a maximum over central/eastern Kansas and Oklahoma. Figure 4 displays a set of back trajectories initialized within the region of enhanced LNO_x. These trajectories link the LNO_x maximum to the storms in northeast Colorado and surrounding areas to the north and east that persisted from 2200 UT 7 June to 0900 UT 8 June producing an estimated 88,421 total flashes.

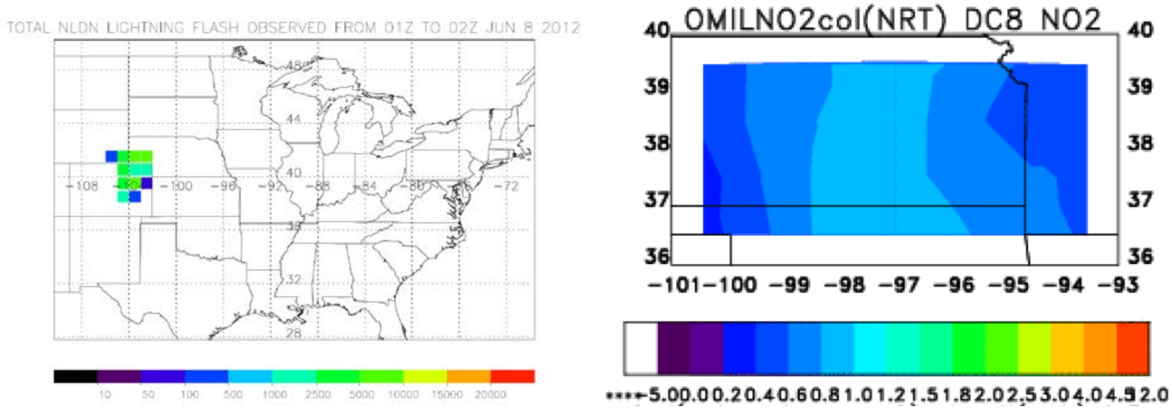

Figure 3. (left) Gridded total flash counts derived from NLDN cloud-to-ground flashes scaled using climatological IC/CG ratios for the period 0100 – 0200 UT on 8 June 2012; (right) OMI LNO_2 maximum over Kansas and Oklahoma at ~1830 UT on 8 June 2012. Units: 10^{15} molecules cm^{-2}.

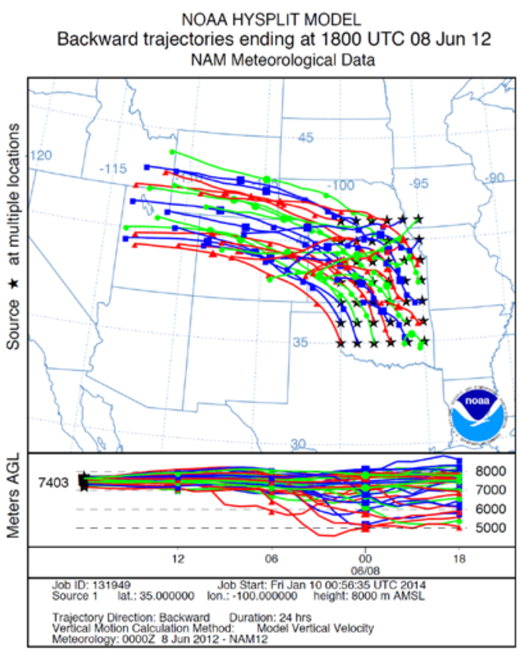

Figure 4. Back trajectories from region of LNO_x enhancement on 8 June 2012, indicating transport from Colorado/Wyoming/Nebraska storms in the 8 km layer.

Active Convection Cases

Analysis of OMI LNO_x from two active convection cases is underway. Figure 5 shows the retrieved OMI LNO_2 for 11 June 2012 over storms in Missouri, Arkansas, and Illinois, and the gridded estimated total flashes for the three-hour period from 1400 – 1700 UT, ending about 1.5 hours prior to OMI overpass. Flashes over the period from 1100 UT to overpass time totaled

165,551. Figure 6 shows the OMI LNO_2 for the case of active convection over southern Missouri, Illinois, and Indiana on 21 June 2012.

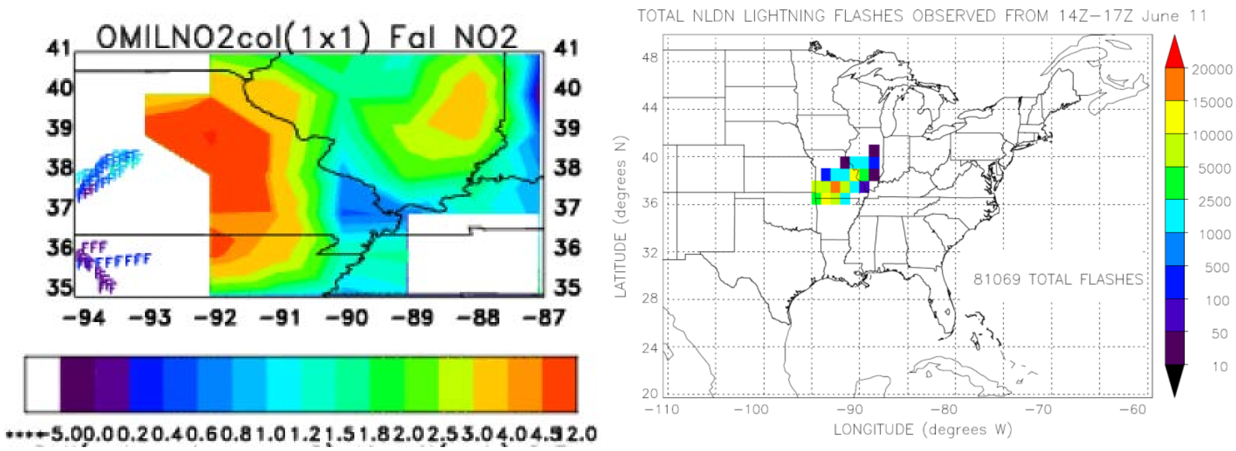

Figure 5. (left) OMI LNO_2 over active convection on 11 June 2012. Units: 10^{15} molecules cm^{-2}. (right) Gridded total flash counts derived from NLDN cloud-to-ground flashes scaled using climatological IC/CG ratios for the period 1400 - 1700 UT on 8 June 2012 (prior to OMI overpass).

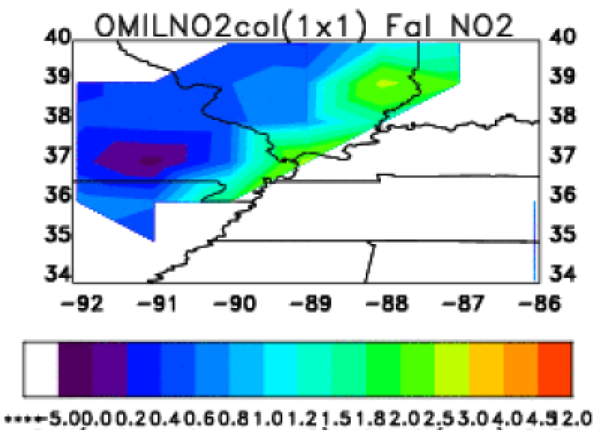

Figure 6. OMI LNO_2 over active convection on 21 June 2012. Units: 10^{15} molecules cm^{-2}.

SUMMARY

Four cases of enhanced LNO_x detected by the OMI instrument on NASA's Aura satellite during the DC3 experiment are being analyzed in relation to the number of contributing flashes in order to make estimates of mean LNO_x production per flash. In each of these cases DC3 research aircraft measured in situ NO_x, providing data with which our satellite retrieval method could be refined. In two cases the enhanced LNO_x was located well downwind of storms, and the enhanced LNO_x region was linked to the contributing flashes by means of air trajectories. For the 29-30 May 2012 Oklahoma convection case, the enhanced LNO_x was found over the southern Appalachians. The number of contributing flashes was determined from a combination of Oklahoma LMA and NLDN data, yielding an estimate of ~280 moles LNO_x per flash, which is well within the range found in the literature. Work is ongoing for case downwind of substantial convection over northeast Colorado and surrounding area and for two cases of active convection over the Arkansas to Indiana region.

ACKNOWLEDGMENTS

This research was supported by the NASA Aura Science Team project. NLDN data are collected by Vaisala, Inc. and archived by NASA Marshall Space Flight Center.

REFERENCES

Beirle, S., N., et al. (2006), Estimating the NOx produced by lightning from GOME and NLDN data: A case study in the Gulf of Mexico, *Atmos. Chem. Phys.*, *6*, 1075–1089.

Beirle, S., H. Huntrieser, and T Wagner (2010), Direct satellite observation of lightning-produced NOx, *Atmos. Chem. Phys*., 10(22), 10965-10986, doi:10.5194/acp-10-10965.

Boccippio, D., K. Driscoll, W. Koshak, R. Blakeslee, W. Boeck, D. Mach, D. Buechler, H. J. Christian, and S. J. Goodman (2000), The Optical Transient Detector (OTD): Instrument Characteristics and Cross-Sensor Validation, *J. Atmos. Oceanic Tech.*, *17*, 441-458.

Boccippio, D. J., W. J. Koshak, and R. J. Blakeslee (2002), Performance assessment of the Optical Transient Detector and Lightning Imaging Sensor, I: Predicted diurnal variability, *J. Atmos. Oceanic Technol.*, *19*, 1318–1332

Bucsela, E. J., K. E. Pickering, et al. (2010), Lightning-generated NOx seen by OMI during NASA's TC4 experiment, *J. Geophys. Res*., doi:10.1029/2009JD013118, in press.

Bucsela, E. J., N. A. Krotkov, E. A. Celarier, L. N. Lamsal, W. H. Swartz, P. K. Bhartia, K. F. Boersma, J. P. Veefkind, J. F. Gleason, and K. E. Pickering, (2013) A new stratospheric and tropospheric NO2 retrieval algorithm for nadir-viewing satellite instruments: applications to OMI, *Atmos. Meas. Tech. Discuss*., 6, 1361–1407, www.atmos-meas-tech-discuss.net/6/1361/2013/doi:10.5194/amtd-6-1361-2013.

Christian, H. J., et al. (2003), Global frequency and distribution of lightning as observed from space by the Optical Transient Detector, *J. Geophys. Res.*, *108* (D1), 4005, doi:10.1029/2002JD002347.

DeCaria, A. J., K. E. Pickering, G. L. Stenchikov, and L. E. Ott (2005), Lightning-generated NOx and its impact on tropospheric ozone production: A three-dimensional modeling study of a STERAO-A thunderstorm, *J. Geophys. Res*., *110*, D14303, doi:10.1029/2004JD005556.

Huntrieser, H., U. Schumann, H. Schlager, H. Höller, A. Giez, H.-D. Betz, D. Brunner, C. Forster, O. Pinto Jr., and R. Calheiros (2008), Lightning activity in Brazilian thunderstorms during TROCCINOX: Implications for NOx production, *Atmos. Chem. Phys.*, *8*, 21–953.

Huntrieser, H., et al. (2009), NOx production by lightning in Hector: first airborne measurements during SCOUT-O3/ACTIVE, *Atmos. Chem. Phys*., 9, 8377-8412

Huntrieser, H., H. Schlager, M. Lichtenstern, M., P. Stock, T. Hamburger, H. Höller, K. Schmidt, H.-D. Betz, A. Ulanovsky, and F. Ravegnani (2011), Mesoscale convective systems observed during AMMA and their impact on the NOx and O-3 budget over West Africa, *Atmos. Chem. Phys.*, 11, 2503-2536, doi:10.5194/acp-11-2503.

IPCC (2007), *Contribution of Working Group I to the Fourth Assessment Report of the Intergovernmental Panel on Climate Change*, 2007, S.
Solomon, D. Qin, M. Manning, Z. Chen, M. Marquis, K.B. Averyt, M. Tignor and H.L. Miller (eds.), Cambridge University Press, Cambridge, United Kingdom and New York, NY, USA.

Koshak, W., H. Peterson, A. Biazar, M. Khan, and L. Wang (2013), The NASA Lightning Nitrogen Oxides Model (LNOM): Application to air quality modeling, *Atmos. Res.*, http://dx.doi.org/10.1016/j.atmosres.2012.12.015.

Mach, D. M., H. J. Christian, R. J. Blakeslee, D. J. Boccippio, S. J. Goodman, and W. L. Boeck (2007), Performance assessment of the Optical Transient Detector and Lightning Imaging Sensor, *J. Geophys. Res.*, *112*, D09210, doi:10.1029/2006JD007787.

Ott, L. E., K. E. Pickering, G. L. Stenchikov, H. Huntrieser, and U. Schumann (2007), Effects of lightning NOx production during the 21 July European Lightning Nitrogen Oxides Project storm studied with a three-dimensional cloud-scale chemical transport model, *J. Geophys. Res.*, *112*, D05307, doi:10.1029/2006JD007365.

Ott, L. E., K. E. Pickering, G. L. Stenchikov, D. J. Allen, A. J. DeCaria, B. Ridley, R.-F. Lin, S. Lang, and W.-K. Tao (2010), Production of lightning NOx and its vertical distribution calculated from three-dimensional cloud-scale chemical transport model simulations, *J. Geophys. Res*., *115*, D04301,doi:10.1029/2009JD011880.

Price, C., J. Penner, and M. Prather (1997), NOx from lightning 1. Global distribution based on lightning physics, *J. Geophys. Res*., *102* (D5), 5929-5941.

Schumann, U., and H. Huntrieser (2007), The global lightning-induced nitrogen oxides source, *Atmos. Chem. Phys*., *7*, 3823-3907.

Wang, Y., A. W. DeSilva, G. C. Goldenbaum, and R. R. Dickerson (1998), Nitric oxide production by simulated lightning: Dependence on current, energy and pressure, J. *Geophys. Res.*, 103, 19,149– 19,159.

Zhang, R., X. Tie, and D. W. Bond (2003), Impacts of anthropogenic and natural NOx sources over the U.S. on tropospheric chemistry, *Proc. Natl. Acad. Sci. U.S.A.*, *100* (4), 1505-1509, doi:10.1073/pnas.252763799. Abarca, S. F. K. L. Corbosiero, and T. J. Galameau Jr. (2010), An evaluation of the WWLLN using the NLDN as ground truth, *J. Geophys. Res*., 115, D18206, doi:10.1029/2009JD013411.